Application Note

Laplace Deep Level Transient Spectroscopy using the MFIA

Zurich Instruments

Applications: Impedance
Products: MFIA

Release date: Aug 2017

Introduction

Deep Level Transient Spectroscopy (DLTS) is a powerful tool for characterizing electrically active majority carrier traps in semiconductors [1]. The basic principle of DLTS consists of measuring the capacitance of a suitable junction such as a reverse-biased Schottky diode, while filling biasing voltage pulses are applied.

The voltage pulses sweep the majority carriers into the volume of the junction, which is initially depleted of mobile charge carriers due to reverse biasing. Here, they may be captured by electrically active defects. After restoring the initial reverse biasing, the trapped majority carriers are progressively emitted from the electrically active defects, causing a gradual change in capacitance. Measuring this capacitance transient provides a fingerprint of the defects involved in the emitting process.

The amplitude of the transient is related to the concentration of the defects, while the time constant is related to their energy level of the defect and capture cross section. Various numerical procedures exist for extracting these defect properties from the measured capacitance transient. This note presents two fundamentally different procedures: conventional-DLTS (henceforth DLTS) and Laplace-DLTS (L-DLTS). In the case of DLTS, the acquired signal is multiplied by a weighting function and the output integrated over time, thus resulting in a maximum when the transient time constant corresponds to a known preset value, the so called “rate window”. In the case of L-DLTS, the Laplace reverse transform of the measured transient is numerically calculated to extract the spectral density and to distinguish individual contributions within the acquired data. This note describes an MFIA-based setup used to perform the DLTS and L-DLTS measurements, and compares its performance with a commercially available DLTS/L-DLTS system based on the Boonton 7200 [2]. The results shows that the MFIA-based setup performs at least on par with the Boonton-based setup. Finally, this note summarizes some key differences between DLTS and L-DLTS, and shows that L-DLTS can be considered as a refinement to DLTS.

Setup and Sample

A description of the setup used to perform the DLTS and L-DLTS characterization is given in Figure 1. The capacitance was measured in a 4-terminal configuration using the MFIA in the 3 V and 1 mA voltage and current range, respectively. An internal DC offset, V_{dc} , of -2.8 V was added to the 30 mV_{rms} test signal, V_{test}, in order to reverse bias the Schottky diode. The negative biasing DC voltage, V_{dc}, was superimposed with 100 ms pulses of 2.8 V (V_p) supplied by a pulse generator (Agilent 33220A) and fed into Aux Input 1 of the MFIA. In addition, the sync signal output of the pulse generator was connected to the MFIA back panel Trigger Input 1 in order to synchronize pulse generation with transient acquisition. The MFIA was controlled, and data was acquired, using LabView.

The sample consists of a Pd-ZnO Schottky diode realized on a hydrothermally grown ZnO wafer (n-type) [3]. It was installed in a liquid nitrogen cryostat connected to a Lakeshore 332 temperature controller. Due to significant spurious impedance of the custom fixture and wiring, a compensation step was performed prior to acquiring the transients. It is also worth mentioning that, no 180° phase shifted signal was added to compensate the constant capacitance component of the Pd-ZnO Schottky diode. This is in contrast to the method reported in the previous blogpost describing DLTS measurements [1]. In this note, the total

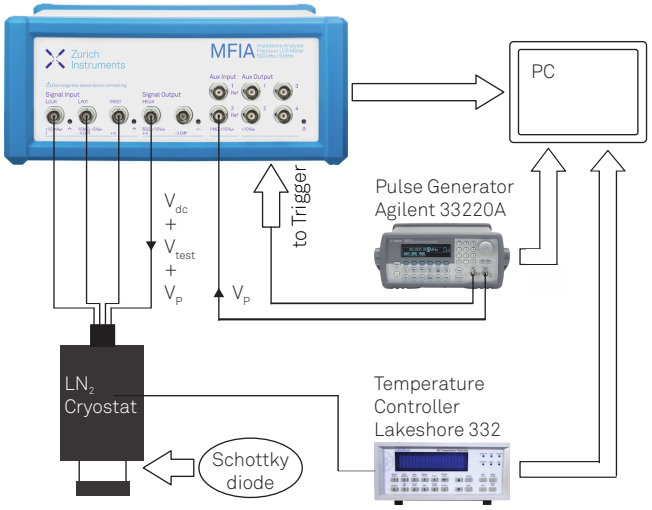

Figure 1. Schematic view of the MFIA-Based DLTS set-up.

sample capacitance was measured during the DLTS/L-DLTS characterization while using the MFIA without any voltage-overflow conditions occurring even when the filling pulse was present (this condition has been found to be crucial for optimal performance).

DLTS with the MFIA

MFIA vs Boonton 7200

A thorough study was carried out to compare the measurements performed with the MFIA-based setup described in Figure 1 and a commercially available DLTS setup based on a Boonton 7200 capacitance meter [2]. Transients acquired with these two setups, under equal quiescent conditions (V_{dc}= -2.8 V, V_p = 2.8 V for 100 ms) and capacitance signal sampling rate (13 kHz) are shown in Figure 2 (a) and (b). Figure 2 shows very good agreement between the two setups for the acquired capacitance, including a similar signal-to-noise ratio, SNR. No overflow condition occurs when the pulse is applied while using the MFIA, so the capacitance is also accurately measured during the pulsing release, as shown in Figure 2 (a) and (b). On the contrary, for the measurements performed with the Boonton 7200 a recovery time of ~0.2 ms is observed as a consequence of the overloading during the pulsing time.

Having established the MFIA-based setup performs well compared with the Boonton-based one, a more detailed analysis was performed using the MFIA-based setup. If only one kind of trap with concentration (N_t) is present in the Schottky diode depletion region, the time, t, and temperature, T, dependence of the capacitance transients, $\Delta C(T,t)$, is equal to [4]

$$\frac{\Delta C(T,t)}{C_0} = -\frac{N_t}{2N_d} exp\left(-e_n\left(T\right)t\right) \cdot F(T, V_{DC}, V_p) \quad (1)$$

where C_0, N_d and e_n(T) are the quiescent capacitance of the Schottky diode, donor concentration and the

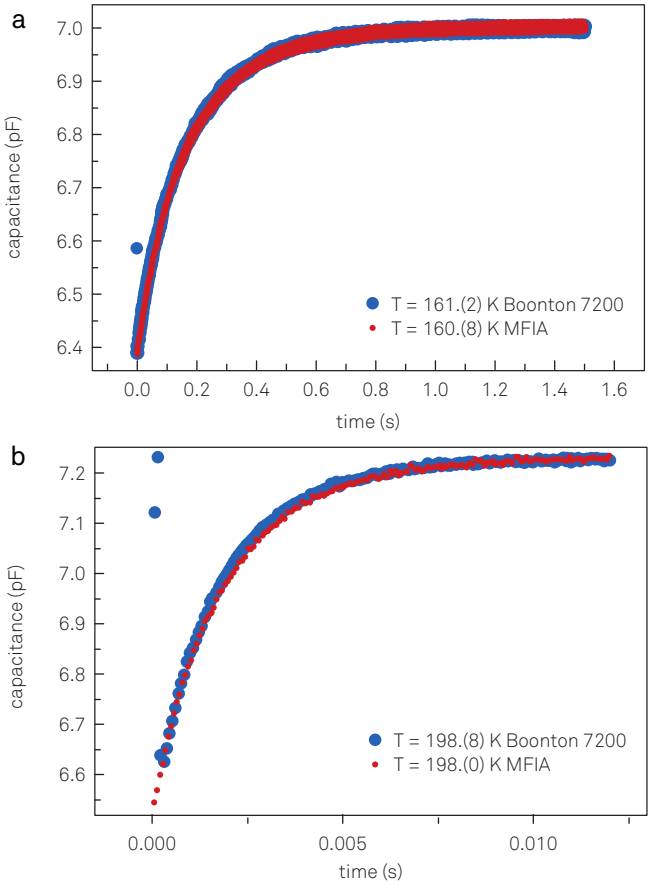

Figure 2. Capacitance transients acquired at 1 MHz, sampling rate 13 kHz, and temperature ~161 K (a) and ~198 K (b) using the MFIA (red dots) and Boonton 7200 in the 2 pF range (blue dots). Data points related to the recovery time from overloading are present on the Boonton 7200 measurements, but the MFIA is not affected.

emission rate, respectively, while F is a correcting factor (~1 in ordinary measurements conditions), that takes into account the actual portion of depletion region investigated during the measurements [4, 5, 6].

DLTS vs L-DLTS

In DLTS, capacitance transients are acquired while the temperature is ramped up or down. The DLTS spectra as a function of temperature, $S(T)$, is obtained by filtering the transient capacitance, averaged in a temperature interval around T, with a weighting function, $W(t)$ i.e. by performing the following integral:

$$S\left(T\right) = \frac{1}{t_w}\int_{t_d}^{t_d+t_w} W(t)\Delta C\left(T,t\right)dt \quad (2)$$

where t_d and t_w are the delay time (introduced to eliminate the impedance meter overloading) and the time length of the time window, respectively. A maximum in $S(T)$ is obtained when e_n(T) matches the filter window corresponding to the $W(t)$ chosen. Furthermore, from the DLTS spectra peak height $2\Delta C/\ C_0$ can be extracted by inverting Equation 2. This quantity is approximately equal to the ratio of defect to main donor concentration as can be deduced by looking at Equa-

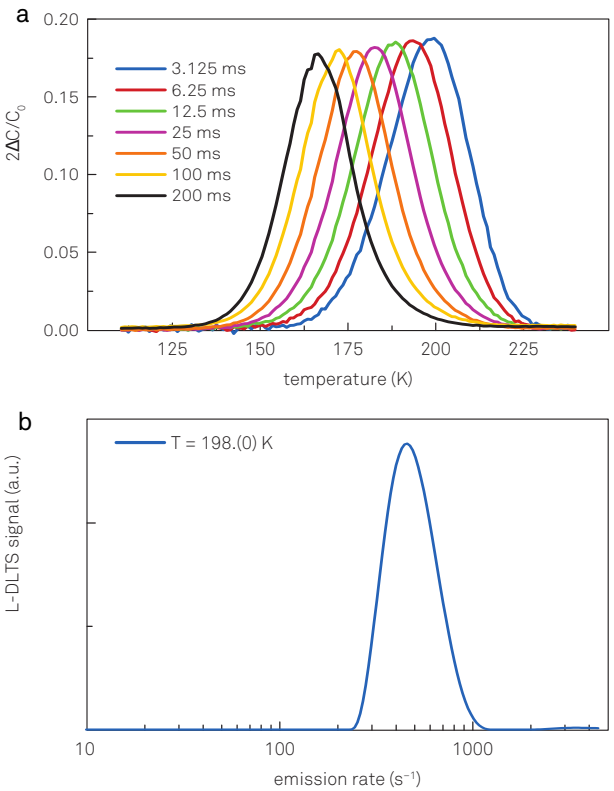

Figure 3. DLTS (a) and L-DLTS (b) spectra acquired with V_{dc} = -2.8 V, V_p = 2.8 V for 100 ms and capacitance measured at 1 MHz with a sampling rate of 13 kHz. In (a) curves correspond to the different time window lengths, t_w, used for W(t) to analyze transients (t_d = 4 x 10^{-4} s in all the measurements). A maximum can be observed occurring, for example, at 198 K for a window length of 3.125 ms. In (b) an L-DLTS spectrum obtained by performing a Laplace numerical inversion of an averaged capacitance transient acquired at T ~198K.

tion 1. The DLTS spectra and an example of such analysis is shown in Figure 3 (a) were obtained by using the following weighting function:

$$W(t) = \begin{cases} -1 & t_d \le t < t_d + t_w/2 \\ 1 & t_d + t_w/2 \le t \le t_d + t_w \end{cases} \quad (3)$$

Such a function has the characteristic that the maximum will occur when $e_n(T) \sim (t_w/2)^{-1}$. It is also worth pointing out that filtering with this weighting function is essentially the difference between the transient averaged over the first and the second half of the time window length. Therefore, this approach has the advantage of significantly reducing the noise contribution and increasing sensitivity. As an example, the longest time window acquisition shown in Figure 3(a) consists of 2500 points. As a consequence of this integration, the SNR is increased by a factor $\sqrt{\frac{2500}{2}} \sim 30$ when performing the integrals over the time interval $t_W/2$. This implies a factor ~20 higher SNR in the resulting DLTS spectrum.

By applying the weighting function from Equation 3 to the measured transients, a maximum at 198 K was observed for a window length of 3.125 ms as shown in Figure 3 (a). This peak indicates the presence of defects. L-DLTS provides another possible approach to analyze

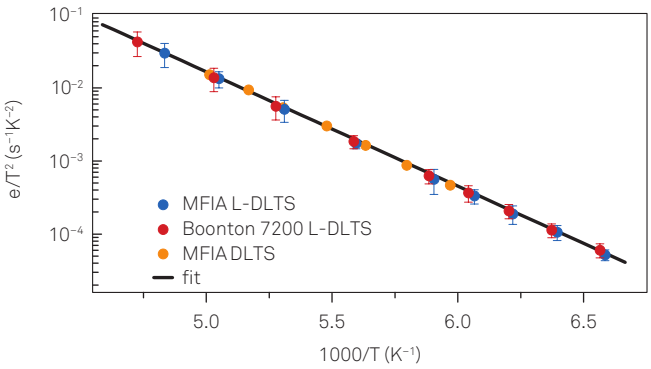

Figure 4. Arrhenius plot used to extract the defect activation enthalpy and apparent capture cross section. Data obtained by L-DLTS transient analysis and DLTS are shown.

the acquired transients. For a given transient, the emission rate spectral distribution is obtained by numerically solving the integral:

$$\Delta C(T,t) = \int_0^{+\infty} F(s(T))\, e^{-s(T)t} ds \quad (4)$$

i.e. computing the reverse Laplace transform. This involves discretization of the integral equation and the solution of the system of equations so obtained. The weighting function integration can be generally considered as a smoothing operation. On the contrary, solving Equation 4 requires inverting the integral. This is a Fredholm integral equation of the first kind, which is an ill-posed problem meaning the solution is not stable in the presence of the noise accompanying the $\Delta C(T,t)$ measurements. Furthermore, in such conditions there may be no or an infinite number of solutions. Therefore, a regularization method which smooths the minimizing procedure is required to search for the stable and most probable solution. For the same reason from an experimental point of view, to successfully perform the Laplace inverse transform, a high SNR is required, typically of the order of 1000 when the Tikhonov regularization is used [7]. Such a high SNR can be achieved by acquiring a large number (generally in the range of 100 - 1000) of transients at fixed temperature and averaging them prior to performing the numerical analysis. For example, the transients shown in Figure 2 (a) and (b) were obtained by averaging 500 measurements to achieve the target SNR. The Laplace inverse transform calculated using the Transient Processing Utility [2] based on the above-mentioned Tikhonov regularization method for measurements taken at ~198 K confirms the presence of a single main defect and is shown in Figure 3 (b) .

Both DLTS and L-DLTS spectra shown in Figure 3 (a) and (b) provide information on the presence of defect states. Its electrical fingerprints i.e. the enthalpic energy position respect to the conduction band edge, ΔH, and apparent capture cross section, σ_{na}, can be evaluated considering that theoretically, the dependence

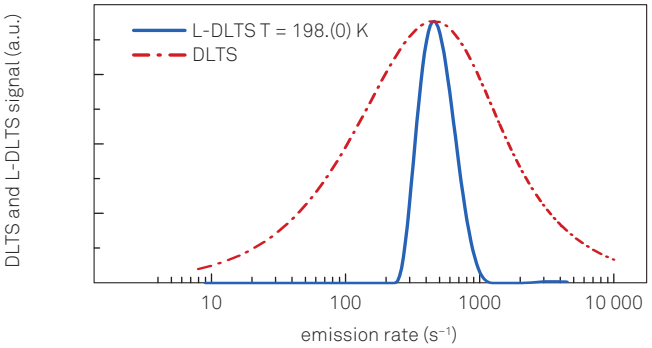

Figure 5. Experimental L-DLTS spectrum extracted from a capacitance transient measured at 198 K (blue trace) and the maximum achievable DLTS resolution calculated for a filtering maximum located at about 450 s^{-1} (red trace).

of e_n(T) on T is given by Equation 5 [4]:

$$e_n(T) = Q\sigma_{na}T^2 \exp\left(-\frac{\Delta H}{kT}\right) \quad (5)$$

where Q is a factor depending on the characteristics of the semiconductor being examined that can be evaluated for ZnO on basis of the literature available. An Arrhenius plot of $e_n(T)/T^2$ vs $1000/T$ can be used to extract the parameters of interest concerning the defect observed. By fitting the data, as shown in Figure 4, a ΔH of (0.310 ± 0.003) eV and σ_{na} of (1.2±0.3)·10^{-16} cm^2 are obtained. These values allow the assignment of the observed defect characteristics to the so called E3 defect commonly observed in ZnO [8].
To illustrate the motivation for introducing the L-DLTS method, the resolution of a lock-in filter centered at ~450 s^{-1} obtained by evaluating the Equation 2 integral as a function of e_n has been calculated. The simulated curve is shown in Figure 5 in comparison with the inverted L-DLTS spectrum (shown also in Figure 3 (b)). This clearly demonstrates the higher resolution of L-DLTS with respect to DLTS; considering the full width at half maximum as the resolution limit, in the case of L-DLTS, transients with a time constant ratio of ~2 can be distinguished, while a ten-times lower resolution is achieved using DLTS. Although it has been shown that L-DLTS resolution is an order of magnitude higher than DLTS, L-DLTS requires a higher SNR and an a-priori knowledge of the temperature interval where the capacitance transient occurs as it is based on isothermal measurements. Therefore, L-DLTS should generally be used as a refinement of the DLTS characterization.

Conclusion

DLTS and L-DLTS spectra have been measured on a setup based on a Zurich Instruments MFIA impedance analyzer, and compared to a system using a Boonton 7200 capacitance meter in its highest resolution range. It has been found that both systems have similar performance at 1 MHz (the fixed working frequency of the Boonton 7200).
Considering the larger flexibility of the MFIA instrument in terms of frequency, test voltage and filtering conditions, this paves the way to perform DLTS measurements by using the described set-up, thus overcoming the limitations of the commonly available commercial DLTS and L-DLTS systems such as overload, recovery time and fixed working frequency.

Acknowledgements

Zurich Instruments would like to thank R. Schifano, K. Gościński, E. Przeździecka and T. A. Krajewski at the Institute of Physics PAS, Warsaw, Poland, for carrying out these measurements, analysing the results and preparing the manuscript.
Project support: UMO- 2016/22/E/ST3/00553, DEC-2013/09/D/ST3/03750, UMO-2013/09/D/ST5/03879 by the Polish National Science Centre (NCN) and PBS2/A5/34/2013 by the Polish National Centre for Research and Development (NCBiR).

References

[1] J Wei. Deep Level Transient Spectroscopy Using HF2LI Lock-in Amplifier. http://www.zhinst.com/blogs/jamesw/deep-level-transient-spectroscopy.

[2] K. Goscinski and L. Dobaczewski. Laplace transform transient processor and deep level spectroscopy http://www.laplacedlts.eu.

[3] R. Schifano; E. V. Monakhov; U. Grossner and B. G. Svensson. Electrical characteristics of palladium schottky contacts to hydrogen peroxide treated hydrothermally grown ZnO. Appl. Phys. Lett., 91:133507, 2007.

[4] P. Blood and J. W. Orton. The Electrical Characterization of Semiconductors: Majority Carriers and Electron States. Academic Press, 1992.

[5] For simplicity, the case of a majority carriers trap and n-type semiconductor has been assumed.

[6] The so called dilute limit, $N_t << N_d$, has to be valid for Equation 1 being fulfilled, as a rule of thumb a N_t / N_d ratio of approximately 10 - 20 percent is generally assumed as upper bound.

[7] L. Dobaczewski; A. R. Peaker; and K. B. Nielsen. Laplace-transform deep-level spectroscopy: the technique and its applications to the study of point defects in semiconductors. J. Appl. Phys., 96:4689, 2004.

[8] F. Schmidt; S. Muller; H. von Wenckstern; G. Benndorf; R. Pickenhain; M. Grundmann. Impact of strain on electronic defects in (Mg, Zn) O thin films. J. Appl. Phys, 116:103703, 2014.